Biochimica et Biophysica Acta 1837 (2014) 1316–1321

Contents lists available at ScienceDirect

Biochimica et Biophysica Acta

journal homepage: www.elsevier.com/locate/bbabio

PSII manganese cluster: Protonation of W2, O5, O4 and His337 in the S1 state explored by combined quantum chemical and electrostatic energy computations ☆

Arturo Robertazzi [1], Artur Galstyan [1], Ernst Walter Knapp *

Department of Biology, Chemistry and Pharmacy, Institute of Chemistry and Biochemistry, Freie Universität Berlin, Fabeckstr. 36a, D-14195 Berlin, Germany

ARTICLE INFO

Article history:
Received 26 November 2013
Received in revised form 17 February 2014
Accepted 29 March 2014
Available online 12 April 2014

Keywords:
PSII
Mn-cluster
Protonation of the OEC
Redox states
pKa

ABSTRACT

Photosystem II (PSII) is a membrane-bound protein complex that oxidizes water to produce energized protons, which are used to built up a proton gradient across the thylakoidal membrane in the leafs of plants. This light-driven reaction is catalyzed by withdrawing electrons from the Mn_4CaO_5-cluster (Mn-cluster) in four discrete oxidation steps [$S_1 - (S_4 / S_0)$] characterized in the Kok-cycle. In order to understand in detail the proton release events and the subsequent translocation of such energized protons, the protonation pattern of the Mn-cluster need to be elucidated. The new high-resolution PSII crystal structure from Umena, Kawakami, Shen, and Kamiya is an excellent basis to make progress in solving this problem. Following our previous work on oxidation and protonation states of the Mn-cluster, in this work, quantum chemical/electrostatic calculations were performed in order to estimate the pKa of different protons of relevant groups and atoms of the Mn-cluster such as W2, O4, O5 and His337. In broad agreement with previous experimental and theoretical work, our data suggest that W2 and His337 are likely to be in hydroxyl and neutral form, respectively, O5 and O4 to be unprotonated. This article is part of a Special Issue entitled: Photosynthesis Research for Sustainability: Keys to Produce Clean Energy.

1. Introduction

Photosystem II is a membrane-bound multi-subunit protein-pigment complex found in cyanobacteria, algae and plants that catalyzes the decomposition of water into protons, electrons and molecular oxygen [1,2]. This light-driven reaction is promoted by the oxygen-evolving complex (OEC). The investigation of the OEC function in PSII is a tremendous challenge for the scientific community [1,2]. Understanding the mechanism would for instance support the development of artificial photosynthetic systems, which could produce oxygen and hydrogen from water with solar power, thus contributing to solve the current world energy problem.

Crystal structures from three different species are to date available with increasing resolutions: 3.8 Å [3], 3.7 Å [4], 3.5 Å [5], 3.0 Å [6], 2.9 Å [7] and, recently, 1.9 Å [8]. In particular the latter high-resolution structure revealed crucial details which were not visible in previous PSII crystal structures. The analysis of the high-resolution PSII crystal structure suggested, for instance, that the OEC is a cubane-like Mn_4CaO_5 cluster (Mn cluster), constituted of a Ca atom and three Mn atoms, bound through four oxygens (O1, O2, O3, O5) as well as an external Mn (Mn4), bound via O5 and a fifth oxygen atom (O4) (Fig. 1). In the high-resolution crystal structure, all ligands of the Mn cluster were determined, four of which identified as water molecules, W1 and W2 bound to Mn4, W3 and W4 bound to Ca [8].

Although the authors of the most recent crystallographic study of PSII claimed that the Mn-cluster was in the dark-stable S_1 state [Mn(III, III, IV, IV)] [8], strong evidence has emerged that a possible X-ray photo-reduction of the Mn-cluster may have occurred during the experiment [9–13]. A recent computational study [13] suggested the hypothesis that the crystal structure may in fact correspond to a mixture of different oxidation states. In a recent study [9], we confirmed this hypothesis by performing extensive density functional theory (DFT) calculations on the most recent high-resolution PSII crystal structure. By analyzing the structural features of different 78 oxidation and protonation states of the Mn-cluster, we confirmed that the excess of electrons generated by synchrotron radiation caused radiation damage of the Mn-cluster.

The protonation pattern of the Mn-cluster is another aspect that is still far from being clarified [2]. This information is, however, crucial to provide an atomic-detailed description of the catalytic mechanism of water oxidation. While O2, O1, and O3 atoms are likely to be unprotonated in the S_1 state [14], protonation of water ligands W1 and W2, as well as that of O4 and O5 and His337 is still a matter of debate. Remarkably, spectroscopic studies suggested that O5 may be one

☆ This article is part of a Special Issue entitled: Photosynthesis Research for Sustainability: Keys to Produce Clean Energy.

* Corresponding author. Tel.: +49 3083854387.
E-mail address: knapp@chemie.fu-berlin.de (E.W. Knapp).

[1] Authors contributed equally.

http://dx.doi.org/10.1016/j.bbabio.2014.03.018
0005-2728/

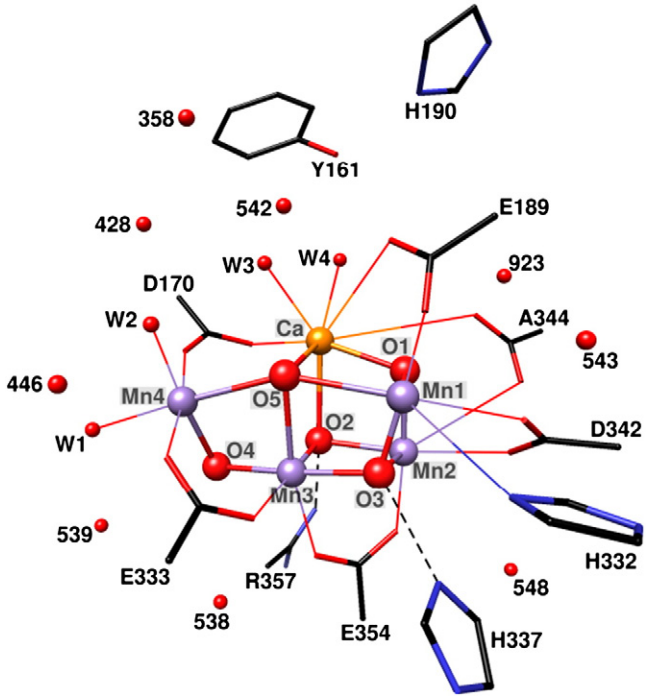

Fig. 1. Oxygen-evolving complex (OEC), the nomenclature of the Mn_4CaO_5-cluster (Mn-cluster).

of the sites for substrate water, indicating that one or more protons may be present at this position [2,15]. Pace and co-workers [16] stated that in the S_0–S_3 states at least one of either O5 or O4 should be protonated. In particular, their findings based on DFT calculations indicate that the best structure (when compared to experimental high-resolution crystal structure) was obtained when O4 was protonated. They also found that their best model is compatible with one of the two Mn4 water ligands being deprotonated. Based on QM/MM computations combined with a comparison to EXAFS spectra, Luber et al. [13] have recently suggested that no proton should be attached to neither O5 nor O4 and that the ligands on Mn4 should be neutral waters, in line with other studies [2,15,17,18]. Using a similar combined DFT/EXAFS approach, Kusunoki [19] explored the possibility for the Mn-cluster to exist in two different isomeric structures in the S_2 state, finding that one of the two water ligands on Mn4 may be in the hydroxyl form. Interestingly, ESEEM and ENDOR studies [18,20] suggested that either W1 or W2 should be deprotonated in the S_2 state. Neese and co-workers confirmed this finding theoretically [15].

In our recent theoretical study [9], the Mn-cluster of PSII in the high-resolution crystal structure was analyzed with extensive quantum chemical computations which involved 78 different models with different protonation patterns and oxidation states. It was concluded that due to radiation damage, the Mn-cluster in the PSII crystal structure is in a highly reduced state, which is most likely S_{-3} with the W2 water ligand deprotonated, two μ-oxo-bridges, namely O4 and O5, protonated as well as His337. However, there are also other quantum chemical computations favoring the S_{-1} state being populated albeit based on a smaller number of considered atoms [13]. In the same study, it was suggested that in the oxidation state S_1 the most likely model of the OEC may bear one or no protons on the O4 and O5 oxygens, W2 ligand being charge neutral and His337 protonated. Regarding His337, Pace et al. [21] have explored the His337$^{\cdots}$O3 H – bond interaction. Although they excluded that O3 is protonated in the S_1 state, they suggested that protonation becomes more likely in more reduced states, in full agreement with our previous studies [9]. If this is true, an extra proton on His337 may be the source for a subsequent protonation of O3.

Based on the most suitable structures obtained in our previous study [9], in this work a series of pKa calculations were performed in order to explore the protonation of the PSII Mn-cluster in the S_1 state. Our results suggest no protons on the μ-oxo bridges, a neutral His337 and W2 ligand to be in the hydroxyl form as the most likely protonation pattern. This work represents the first step to fully determine the protonation pattern of the Mn-cluster. Further studies are currently being carried out employing alternative approaches, such as, for instance, QM/MM calculations and QM/EXAFS calculations.

2. Computational details

To compute the absolute pKa values of the OEC models, a procedure developed in a previous study was employed [22], which demonstrated an accuracy of about 0.55 pKa units for a number of organic compounds. For the deprotonation reaction $HA \rightleftarrows H^+ + A^-$, the pKa is defined as

$$pKa = \frac{\Delta G_R}{2.303 \cdot RT}, \tag{1}$$

where ΔG_R is the free energy of deprotonation reaction.

ΔG_R can be determined from the thermodynamic cycle (Scheme 1) as

$$\Delta G_R = \Delta G_{gas} + \Delta G_{solv}(A^-) + \Delta G_{solv}\left(H^+\right) - \Delta G_{solv}(HA), \tag{2}$$

where $\Delta G_{solv}(A^-)$, $\Delta G_{solv}(H^+)$ and $\Delta G_{solv}(HA)$ are the corresponding solvation energies and ΔG_{gas} is the deprotonation free energy in vacuum:

$$\Delta G_{gas} = G_{gas}(A^-) + G_{gas}\left(H^+\right) - G_{gas}(HA), \tag{3}$$

with $G_{gas}(H^+) = -6.28$ kcal/mol [22]. Solvation energy of the proton $\Delta G_{solv}(H^+)$ was considered to be −265.74 kcal/mol, as suggested in our previous work [22]. The free energy in vacuum can be calculated as follows:

$$G_{gas} = E_0 + ZPE + \Delta G_{0\rightarrow 298\ K} \tag{4}$$

where E_0 is the ground-state electronic energy in vacuum, ZPE the zero-point vibrational energy and $\Delta G_{0\rightarrow 298\ K}$ the thermal vibration free energy at 298 K. E_0, ZPE, and $\Delta G_{0\rightarrow 298\ K}$ were calculated quantum chemically.

All DFT calculations were performed with Jaguar v7.7 [23,24]. Full geometry optimizations were carried out using B3LYP [25–28] functional together with LACVP [29], an effective core potential for metal atoms and 6–31G** basis set for other elements. Vibrational frequencies and electrostatic potentials were calculated from fully optimized structures on the same level of theory. Single-point electronic energy (E_0) calculations were performed on the optimized structures using a more refined approach, including LACV3P [23] effective core potential and 6–311G++** basis set. Due to anti-ferromagnetic coupling between Mn atoms in the OEC, the total spin S = 0 was used, as determined experimentally for S_1 state [30]. Optimized geometries, charges and energies of the studied complexes and reactions are available in the Supporting Information.

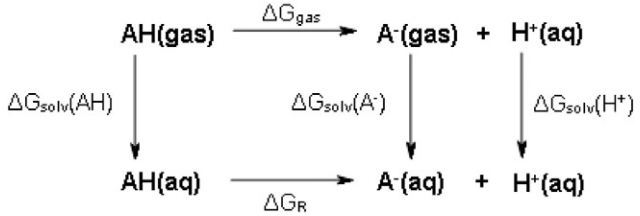

Scheme 1. Thermodynamic cycle to calculate the free energy of deprotonation.

In our solvation model, the protein environment was represented as a dielectric continuum. When the electrostatic behavior of a protein is solely described by dielectric continuum the dielectric constant ranges typically from 10 to 40, depending on the type of protein and its environment [31]. For the protein environment of OEC, the value of $\varepsilon = 20$ was used [32,33]. Solvation energies were calculated by solving Poisson equation using the Solvate module from MEAD program suite [34]. Atomic partial charges were determined from the electrostatic potentials using the restraint-electrostatic-potential (RESP) method as described previously [35]. Van der Waals radii for H, N, O and C were adopted from Ref. [36] and are (in Å) 1.2, 1.4, 1.4 and 2.0, respectively. The values for Mn (1.48 Å) and Ca (1.7 Å) were taken from Jaguar's set of atomic radii [2]. A solvent probe radius of 1.4 Å was used.

2.1. Models

The models employed for DFT calculations include the Mn-cluster with its ligands (Asp170, Glu189, His332, Glu333, Asp342, Ala344, Glu354, HOH540, HOH541, HOH999, HOH1000) together with those near residues (Tyr161, His190, His337, Arg357, HOH358, HOH428, HOH446, HOH538, HOH539, HOH542, HOH543, HOH548, HOH923), which are involved in H-bonds with OEC or its ligands (our notation: W1, W2, W3, W4 corresponds to water ligands HOH1000, HOH999, HOH541 and HOH540, Fig. 1). Amino acids were truncated at specific positions as described elsewhere [9].

Results of our previous work [9] allowed us to focus in this work on mostly relevant protonation states based on Models 1, 2 and 3. These are 1, 1A, 1B, 1C, 2, 2B, 2C, 3, 3B and 3C (see Tables 1 and 2; selected geometrical parameters are displayed in Table S2, Supporting Information). In our nomenclature, the number corresponds to OEC-core protonation, keeping W2 deprotonated ($W2^-$) and His337, protonated at N_ε and N_δ ($His337^+$). The letter in the model name corresponds to appropriate OEC-ligand protonation, according to the following scheme: A ($His337^0$-$W2^-$), B ($His337^0$-$W2^0$), and C ($His337^+$-$W2^0$).

3. Results and discussion

In our previous paper [9], the most likely protonation pattern for the Mn-cluster was suggested based on a careful analysis of geometries and energies from a series of 78 complexes generated from the high-resolution PSII crystal structure through the use of quantum chemical DFT calculations. Our results suggested that the Mn-cluster should bear no protons or one on either O4 or O5. The protonation of water W2 and His337 was also explored. Our data indicated that a hydroxyl form and a protonated His337 are not unlikely. In this work we explore further these preliminary findings by calculating pKa values of the following groups W2, O4, O5 and His337, which are the most promising candidates for alternative protonation pattern found in previous studies [2,9,14,16]. The Mn-cluster models studied in this work are collected in Table 1. The computed pKas are displayed in Table 2 and Fig. 2.

Table 1
List of the Mn-cluster models studied in this work and their protonation pattern.

Model	W2	O4	O5	H337
1	OH^-	O	O	$HisH^+$
1A	OH^-	O	O	His^0
1B	H_2O	O	O	His^0
1C	H_2O	O	O	$HisH^+$
2	OH^-	O	O–H	$HisH^+$
2B	H_2O	O	O–H	His^0
2C	H_2O	O	O–H	$HisH^+$
3	OH^-	O–H	O	$HisH^+$
3B	H_2O	O–H	O	His^0
3C	H_2O	O–H	O	$HisH^+$

Table 2
pKa values of atomic groups and residues considered in the Mn-cluster models. Two different dielectric constants were used, 80 and 20. Reactions marked in bold are depicted in Fig. 2.

Reaction	Residue	pKa (80)	pKa (20)
1C → 1B	H337	4.0	2.1
1 → 1A	H337	2.4	1.5
1C → 1	W2	7.8	6.3
1B → 1A	W2	6.1	5.6
2C → 1C	O5	7.4	4.7
2B → 1B	O5	1.2	−0.8
2 → 1	O5	5.0	3.3
2C → 2B	H337	10.3	7.6
2C → 2	W2	10.3	7.7
3C → 1C	O4	0.2	−2.6
3B → 1B	O4	−7.8	−9.8
3 → 1	O4	5.1	3.4
3C → 3B	H337	12.0	9.3
3C → 3	W2	2.9	0.2

For the pKa computations, two different values of the dielectric constant were employed to mimic the effect of the environment around the models studied in this work. Typically, in electrostatic energy computations of proteins where atomic charges are explicitly taken into account, a value of the dielectric constant between 4 and 20 is used, depending on the model employed for the protein and its application [31]. The more atomic details of the protein model are considered explicitly, the smaller can be the value of the dielectric constant. If no details of the protein are considered except for its volume and shape, an appropriate value is $\varepsilon = 20$ [33]. In this work, protein environment far from the OEC was not considered in atomic detail, therefore $\varepsilon = 20$ was employed to simulate the protein environment. However, considering that the Mn-cluster is surrounded by polar, charged residues and several water molecules, the polarizability in the proximity of the Mn-cluster may be larger than that described by $\varepsilon = 20$. For this reason, also calculations with $\varepsilon = 80$ were performed. Based on our experience [37,38], we estimate the accuracy of the pKa calculations presented in this work to be about 2 pKa units. Results are collected in Table 2 and Fig. 2.

3.1. Protonation state of water ligand W2

Deprotonation of water W2 was explored in the following reactions: 1C → 1, 1B → 1A, 2C → 2, 3C → 3 (Table 2 and Fig. 2). The computed pKa values with $\varepsilon = 20$ are all smaller than 7, except for deprotonation of W2 in Model 2C, for which pKa(20) = 7.7. According to our data, deprotonation of W2 is thus likely to happen, the hydroxyl form of W2 being the most probable. The pKa of W2 is relatively independent of the protonation state of His337. For instance, Model 1B and Model 1C show a similar pKa for W2, pKa(20) = 5.6 and 6.3. More generally the pKa of water W2 ranges between 5.6 and 7.7 except for Model 3C (O4 protonated), in which case pKa(20) = 0.2. These results suggest that a simultaneous protonation of O4 and of His337 can significantly influence the protonation behavior of W2.

3.2. Protonation state of μ-oxo O4

Reactions which feature protonation of O4 are the following: 3C → 1C, 3B → 1B, 3 → 1 (Table 2 and Fig. 2). Computed pKa values for O4-H range between −9.8 and 3.4 at $\varepsilon = 20$, −7.8 and 5.1 at $\varepsilon = 80$. For Models 3B and 3C our data clearly show that protonation of O4 is unlikely, as pKa(20) is close to zero or even negative. Considering that W2 is very likely to be in the OH^- form, analysis of Model 3 becomes more relevant. Model 3 bears a proton on O4,

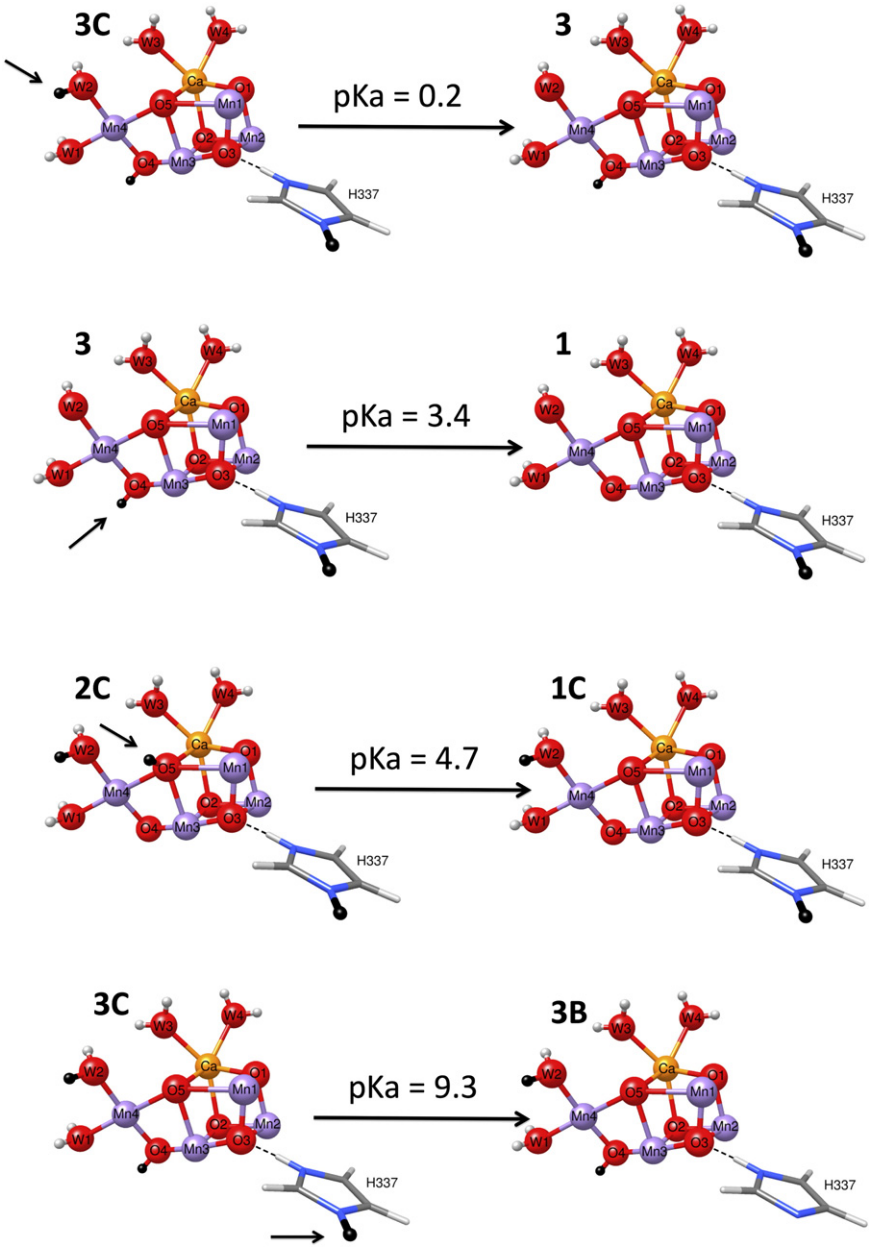

Fig. 2. Most relevant protonation/deprotonation reactions studied in this work, namely W2 and His337 deprotonation, O4 and O5 protonation. All pKa values displayed in the figure are calculated with ε = 20. The relevant protons are highlighted with a black arrow.

W2 in the OH^- form and a protonated His337. The pKa value calculated for O4-H is 3.4 and 5.1 at ε = 20 and ε = 80 respectively.

3.3. Protonation state of μ-oxo O5

Protonation of O5 was considered in the following reactions 2C → 1C, 2B → 1B, 2 → 1 (Table 2 and Fig. 2). The computed pKa values range between −0.8 and 4.7 at ε = 20, 1.2 and 7.4 at ε = 80. Protonation of O5 seems thus to be unlikely for all models, except for Model 2C, which shows a pKa(20) = 4.8 and pKa(80) = 7.4. This in turn means that if His337 is in its neutral state and W2 is H_2O, protonation of O5 may be possible. Remarkably, experimental studies suggested that O5 may be one of the sites for substrate water and thus one or more protons may be present at this position at least transiently [2,15]. In contrast, many theoretical studies provided evidence that no protons should be bound to O5 in the S_1 state [8,13,17,39,40]. In our previous work, we suggested that if a proton is present on the Mn-cluster in S_1, O5 is likely the position that allocates it [9].

3.4. Protonation state of His337

Protonation of His337 was explored in the reactions 3C → 3B, 2C → 2B, 1C → 1B, 1 → 1A. The pKa values of His337 range between 1.5 and 9.3 at ε = 20, while they range between 2.4 and 12.0 at ε = 80. There are thus two types of His337 in the Mn-cluster according to our data. One is represented by Models 3C and 2C, where His337 is likely to be protonated, the other in Models 1C and 1A, in which the His337 pKa values are smaller than 7. While the pKa values are rather independent from the protonation state of W2, protonation of O4 and O5 seems to be crucial for the protonation of His337. When a proton binds either at O4 or O5, the pKa(20) of His337 increases from about 2 to 7.6 and 9.3 for Models 2C and 3C, respectively.

3.5. OEC model for the S_1 state and comparison with literature

The data presented in this contribution suggest that the most likely protonation pattern of the Mn-cluster is that of Model 1A: no protons on O4/O5, W2 ligand is in its OH^- form and His337 is in its neutral form, interacting with O3 via H-bond (Fig. 3). This model is in good agreement with previous experimental and theoretical studies, in particular for the protonation pattern of O5/O4 and W2, for which an abundance of experimental and theoretical studies is available [13,15,17,19,39,40]. For instance, Kusunoki proposed that one of the two water ligands on Mn4 is in fact a hydroxyl [19], in line with ESEEM and ENDOR studies that suggested that in the S_2 state either W1 or W2 should be deprotonated [19] and those of Neese [15], who confirmed theoretically this finding. No proton release is observed in the transition from S_1 to S_2 [14], therefore it is very likely that the W2 ligand is already deprotonated in the S_1 state. Regarding the protonation of O5 and O4, there is a large consensus that these oxygen atoms should be unprotonated [13,15,17,39,40]. We would like to remark that regarding the protonation of His337 in the S2 state of the OEC, Pantazis et al. considered a double protonated histidine in their models, see Supporting Information in Ref. [41].

In our previous paper [9], we stated that O4 and O5 should bear one proton or no protons at all. While this latter hypothesis agrees with our present finding, we still believe that due to the inherent uncertainty of the present pKa computations the possibility that a proton is attached to either O4 or O5 cannot be ruled out. The largest pKa values for protonation at these two oxygens are 4.7 and 3.4 with $\varepsilon = 20$, 7.4 and 5.1 with $\varepsilon = 80$ (Table 2). Since the PSII environment around the Mn-cluster contains a number of water molecules and charged groups and is therefore rather polar, the actual pKa values may be closer to those calculated at $\varepsilon = 80$. Furthermore the uncertainty of the computed pKa values is estimated to be around 2 pKa units. Thus, based on the present study, we cannot exclude protonation on O4 or O5, the latter being slightly more likely.

4. Conclusion

Although the recent high-resolution PSII crystal structure revealed many crucial structural details, protonation of the Mn-cluster is still a matter of debate. A significant number of experimental and theoretical studies focused on this topic [1,2]. In this work, the protonation pattern of the Mn-cluster of PSII was explored by means of pKa calculations carried out at the DFT level combined with continuum electrostatics. In particular, protonation states of water ligand W2, μ-oxo bridges O4 and O5, and of His337 were studied. The studied Mn-cluster structures were chosen from the most relevant models obtained in our previous study on protonation pattern and oxidation states of OEC [9]. The data shown in the present contribution suggested that O4 and O5 are likely unprotonated, since with $\varepsilon = 20$ the pKa values of O5 – H and O4 – H are lower than 7 (Figs. 2 and 3). When no proton is bound to these μ-oxo bridges, our pKa calculations indicate that His337 is very likely deprotonated, i.e. in its charge neutral form (Fig. 3). Moreover, in all studied Mn-cluster models, except Model 2C, W2 is in its hydroxyl form rather than H_2O (Table 2 and Fig. 2). The Mn-cluster protonation pattern obtained in this work (Fig. 2) is in broad agreement with previous findings both based on theoretical and experimental studies [13,15,17,19,39,40].

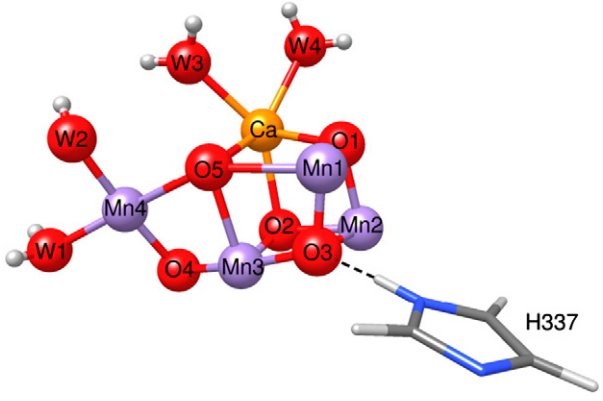

Fig. 3. Model 1A: Most likely Mn-cluster model based on pKa calculations carried out in this study. W2 = OH^-, O5 and O4 unprotonated, His337 in its neutral state.

Despite the broad agreement of the present results with previous studies, there are still uncertain points and open questions. To address these, we are currently carrying out further investigations based on refined pKa calculations (QM/MM and electrostatics) and on a combined DFT/EXAFS approach with the aim of confirming the protonation model presented in this work.

Acknowledgement

A. R. is grateful for having received a Humboldt fellowship. This work is financially supported by project C2 in the Sfb1078 of the Deutsche Forschungsgemeinschaft (DFG).

Appendix A. Supplementary data

Supplementary data to this article can be found online at http://dx.doi.org/10.1016/j.bbabio.2014.03.018.

References

[1] M. Leslie, On the origin of photosynthesis, Science 323 (2009) 1286–1287.
[2] N. Cox, D.A. Pantazis, F. Neese, W. Lubitz, Biological water oxidation, Acc. Chem. Res. 46 (2013) 1588–1596.
[3] A. Zouni, H.T. Witt, J. Kern, P. Fromme, N. Krauß, W. Saenger, P. Orth, Crystal structure of photosystem II from *Synechococcus elongatus* at 3.8 A resolution, Nature 409 (2001) 739–743.
[4] N. Kamiya, J.R. Shen, Crystal structure of oxygen-evolving photosystem II from *Thermosynechococcus vulcanus* at 3.7-A resolution, Proc. Natl. Acad. Sci. U. S. A. 100 (2003) 98–103.
[5] K.N. Ferreira, T.M. Iverson, K. Maghlaoui, J. Barber, S. Iwata, Architecture of the photosynthetic oxygen-evolving center, Science 2004 (1831–1838) 303.
[6] B. Loll, J. Kern, W. Saenger, A. Zouni, J. Biesiadka, Towards complete cofactor arrangement in the 3.0 Å resolution structure of Photosystem II, Nature 438 (2005) 1040–1044.
[7] A. Guskov, J. Kern, A. Gabdulkhakov, M. Broser, A. Zouni, W. Saenger, Cyanobacterial photosystem II at 2.9-A resolution and the role of quinones, lipids, channels and chloride, Nat. Struct. Mol. Biol. 16 (2009) 334–342.
[8] Y. Umena, K. Kawakami, J.-R. Shen, N. Kamiya, Crystal structure of oxygen-evolving photosystem II at a resolution of 1.9 Å, Nature 473 (2011) 55–61.
[9] A. Galstyan, A. Robertazzi, E.W. Knapp, Oxygen-evolving Mn Cluster in Photosystem II: The protonation pattern and oxidation state in the high-resolution crystal structure, J. Am. Chem. Soc. 134 (2012) 7442–7449.
[10] H. Dau, P. Liebisch, M. Haumann, The structure of the manganese complex of Photosystem II in its dark-stable S1-state—EXAFS results in relation to recent crystallographic data, Phys. Chem. Chem. Phys. 6 (2004) 4781–4792.
[11] M. Grabolle, M. Haumann, C. Müller, P. Liebisch, H. Dau, Rapid loss of structural motifs in the manganese complex of oxygenic photosynthesis by X-ray irradiation at 10–300 K, J. Biol. Chem. 481 (2006) 4580–4588.
[12] J. Yano, J. Kern, K.-D. Irrgang, M.J. Latimer, U. Bergmann, P. Glatzel, Y. Pushkar, J. Biesiadka, B. Loll, K. Sauer, J. Messinger, A. Zouni, V.K. Yachandra, X-ray damage to the Mn4Ca complex in single crystals of Photosystem II studied using in situ X-ray spectroscopy: a case study for metallo-protein crystallography, Proc. Natl. Acad. Sci. U. S. A. 102 (2005) 12047–12052.
[13] S. Luber, I. Rivalta, Y. Umena, K. Kawakami, J.R. Shen, N. Kamiya, G.W. Brudvig, V.S. Batista, S1-state model of the O2-evolving complex of Photosystem II, Biochemistry 50 (2011) 6308–6311.
[14] K. Saito, H. Ishikita, Influence of the Ca2+ ion on the Mn4Ca conformation and the H-bond network arrangement in Photosystem II, Biochim. Biophys. Acta 2014 (1837) 159–166.
[15] W. Ames, D.A. Pantazis, V. Krewald, N. Cox, J. Messinger, W. Lubitz, F. Neese, Theoretical evaluation of structural models of the S2 state in the oxygen evolving complex of Photosystem II: protonation states and magnetic interactions, J. Am. Chem. Soc. 133 (2011) 19743–19757.
[16] S. Petrie, P. Gatt, R. Stranger, R.J. Pace, Modelling the metal atom positions of the Photosystem II water oxidising complex: a density functional theory appraisal of the 1.9 Å resolution crystal structure, Phys. Chem. Chem. Phys. 14 (2012) 11333–11343.

[17] P.E.M. Siegbahn, Structures and energetics for O2 formation in Photosystem II, Acc. Chem. Res. 2009 (1871–1880) 42.
[18] C.P. Aznar, D.R. Britt, Simulations of the (1)H electron spin echo-electron nuclear double resonance and (2)H electron spin echo envelope modulation spectra of exchangeable hydrogen nuclei coupled to the S(2)-state photosystem II manganese cluster, Phil. Trans. R. Soc. B 357 (2002) 1359–1366.
[19] M. Kusunoki, S1-state Mn4Ca complex of Photosystem II exists in equilibrium between the two most-stable isomeric substates: XRD and EXAFS evidence, J. Photochem. Photobiol. B 104 (2011) 100–110.
[20] L. Rapatskiy, N. Cox, A. Savitsky, W.M. Ames, J. Sander, M.M. Nowaczyk, M. Ragner, A. Boussac, F. Neese, J. Messinger, W. Lubitz, Detection of the water-binding sites of the oxygen-evolving complex of Photosystem II Using W-Band 17O Electron, ÄìElectron double resonance-detected NMR spectroscopy, J. Am. Chem. Soc. 134 (2012) 16619–16634.
[21] S. Petrie, P. Gatt, R. Stranger, R.J. Pace, The interaction of His337 with the Mn4Ca cluster of photosystem II, Phys. Chem. Chem. Phys. 14 (2012) 4651–4657.
[22] M.S.a. Busch, E.W. Knapp, Accurate pk(a) determination for a heterogeneous group of organic molecules, ChemPhysChem 5 (2004) 1513–1522.
[23] Jaguar 7.7, Schrödinger, L.L.C., New York, 2010.
[24] A.D. Bochevarov, E. Harder, T.F. Hughes, J.R. Greenwood, D.A. Braden, D.M. Philipp, D. Rinaldo, M.D. Halls, J. Zhang, R.A. Friesner, Jaguar: a high-performance quantum chemistry software program with strengths in life and materials sciences, Int. J. Quantum Chem. 113 (2013) 2110–2142.
[25] A.D. Becke, Density-functional exchange-energy approximation with correct asymptotic behavior, Phys. Rev. A 38 (1988) 3098–3100.
[26] C. Lee, W. Yang, R.G. Paar, Development of the Colle-Salvetti correlation-energy formula into a functional of the electron density, Phys. Rev. B 37 (1988) 785–789.
[27] J.C. Slater, Quantum theory of molecules and solids, vol. 4McGraw-Hill, New York, 1974.
[28] S.H. Vosko, L. Wilk, M. Nusair, Accurate spin-dependent electron liquid correlation energies for local spin density calculations: a critical analysis, Can. J. Phys. 58 (1980) 1200–1211.
[29] P.J. Hay, W.R. Wadt, Ab initio effective core potentials for molecular calculations. Potentials for K to Au including the outermost core orbitals, J. Chem. Phys. 82 (1985) 299–310.
[30] D. Koulougliotis, D.J. Hirsh, G.W. Brudvig, The oxygen-evolving center of photosystem II is diamagnetic in the S1 resting state, J. Am. Chem. Soc. 114 (1992) 8322–8323.
[31] M. Gilson, B. Honig, The dielectric constant of a folded protein, Biopolymers 25 (1986) 2097–2119.
[32] C.N. Schutz, A. Warshel, What are the dielectric "constants" of proteins and how to validate electrostatic models? Proteins 44 (2001) 400–417.
[33] A. Galstyan, S.D. Zaric, E.W. Knapp, Computational studies on imidazole heme conformations, J. Biol. Inorg. Chem. 10 (2005) 343–354.
[34] D. Bashford, K. Gerwert, Electrostatic calculations of the pKa values of ionizable groups in bacteriorhodopsin, J. Mol. Biol. 224 (1992) 473–486.
[35] A. Galstyan, E.W. Knapp, Accurate redox potentials of mononuclear iron, manganese, and nickel model complexes, J. Comput. Chem. 30 (2009) 203–211.
[36] M. Schmidt am Busch, E.W. Knapp, Accurate pKa determination for a heterogeneous group of organic molecules, ChemPhysChem 5 (2004) 1513–1522.
[37] G.M. Ullmann, E.W. Knapp, Electrostatic models for computing protonation and redox equilibria in proteins, Eur. Biophys. J. 28 (1999) 533–551.
[38] B. Rabenstein, E.W. Knapp, Problems evaluating energetics of electron transfer from QA to QB: the light exposed and dark-adapted bacterial reaction center, Molecular Bioenergetics, American Chemical Society, vol. 883, 2004, pp. 71–92.
[39] E.M. Sproviero, J.A. Gascón, J.P. McEvoy, G.W. Brudvig, V.S. Batista, Quantum mechanics/molecular mechanics study of the catalytic cycle of water splitting in photosystem II, J. Am. Chem. Soc. 130 (2008) 3428–3442.
[40] A. Grundmeier, H. Dau, Structural models of the manganese complex of Photosystem II and mechanistic implications, Biochim. Biophys. Acta 2012 (1817) 88–105.
[41] D.A. Pantazis, W. Ames, N. Cox, W. Lubitz, F. Neese, Two interconvertible structures that explain the spectroscopic properties of the oxygen-evolving complex of Photosystem II in the S2 state, Angew. Chem. Int. Ed. Engl. 51 (2012) 9935–9939.